Hindawi
Shock and Vibration
Volume 2018, Article ID 5064930, 18 pages
https://doi.org/10.1155/2018/5064930

Research Article

Statistical Analysis of Wind-Induced Dynamic Response of Power Towers and Four-Circuit Transmission Tower-Line System

Xiaolei Zhang, Yanzhong Ju, and Fuwang Wang

Northeast Electric Power University, 169 Changchun Rd., Chuanying District, Jilin 132012, China

Correspondence should be addressed to Xiaolei Zhang; xiaolei_052@sina.com

Received 29 July 2017; Revised 4 January 2018; Accepted 7 February 2018; Published 12 March 2018

Academic Editor: Giuseppe Carlo Marano

Only one wind field model loading the transmission tower or the tower-line system was investigated in the previous studies, while the influence of two different wind field models was not considered. In addition, only one sample of the wind speed random process was used in the past numerical simulations, and the multiple dynamic response statistical analysis should be carried out. In this paper, statistical analysis of the wind-induced dynamic response of single towers and the transmission tower-line system is performed with the improved accuracy. A finite element model of the transmission tower-line system (the tower consisted of both steel tubes and angel steels) is established by ANSYS software. The analysis was performed by three statistical methods. The effects of the length of the time history and of the number of samples were investigated. The frequency histograms of samples follow the Gaussian distribution. The characteristic statistical parameters of samples were random. The displacements and the axial forces of the low tower are larger than those of the high tower. Two wind field models were applied to simulate the wind speed time history. In field 1 model, Davenport wind speed spectrum and Shiotani coherence function were applied, while in field 2 model Kaimal wind speed spectrum and Davenport coherence function were used. The results indicate that wind field 1 is calmer than wind field 2. The displacements and the axial forces of the tower-line system are less than those of single towers, which indicate damping of wind-induced vibrations by the transmission line. An extended dynamic response statistical analysis should be carried out for the transmission tower-line system.

1. Introduction

The power transmission tower-line system is a complex spatial coupled vibration system. Vibration is the main cause of damage to the power circuits [1–4]. Because of the high flexibility of power towers and the geometrical nonlinearity of the conductor and insulator strings, it is difficult to simulate precisely the dynamic response of a tower-line system. Usually, the transmission line and the towers were analyzed independently, the coupling effect of the line and tower was ignored; thus, the calculation analysis was inaccurate [5–8].

The wind response of the power transmission tower-line systems has been considered in a series of studies. Mara and Hong [9] performed a numerical simulation to investigate the effect of wind direction on the response and the surface capacity of a lattice transmission tower under wind loads. The inelastic response parameters and the capacity curve for a single tower were calculated in the paper. Yang et al. [10, 11] developed the three-dimensional finite element models of UHV single anchor tower and the tower-line system and analyzed the responses of the anchor tower and tower-line system under a wind load. The results show that the displacement, the axial force, and the main column counteracting force have a nonlinear change trend with the initial stress increase. Under a wind load, the mean displacement and the maximum axial force on anchor tower are much higher than those under the equivalent static load. Chen et al. [12] and Aboshosha and El Damatty [13] emphasized that the influence of dynamic interaction of the conductor and ground wires on towers needs to be investigated. Zhou et al. [14, 15] introduced the theory of rain wind-induced vibration on the stay cable in transmission line.

Table 1: Types and parameters of lines.

	Conductor line	Ground line
Type	JLHA2/LB14-630/45	JLHA2/LB14-95/55
A (mm2)	666.6	152.8
d (mm)	33.6	16
q (kg/km)	2030	670
T_{cp} (N)	58116	26120
T_{max} (N)	77488	32650
E (MPa)	62400	97400
α (1/°C)	$21 * 10^{-6}$	$15.6 * 10^{-6}$

Hamada et al. [16–20] developed a nonlinear three-dimensional four-nodded cable element and the nonlinear three-dimensional numerical model to simulate the transmission line and towers behaviour. They studied the progressive failure of the lattice transmission tower-line systems under tornado wind loads and proved the importance of the transmission lines in the analysis of transmission tower-line systems under tornado loads. Tian and Zeng [21] carried out a parametric study of tuned mass dampers for a long span transmission tower-line system under wind loads. Barbosa et a1. [22] proposed a methodology for the reduction of faults in transmission tower-line system under high-speed wind events and gusts, including a safety analysis and recommendations for corrective maintenance. The above researchers mainly focused on either angle steel tower or the steel tube tower, while towers consisted of both steel tubes and angel steels were less investigated. Therefore, the coupling effect of the tower-line system on the wind vibration response should also be considered for the case of the tower which consisted of both steel tubes and angel steels. It should be noted that only one wind field model loading the transmission tower or the tower-line system was investigated in the previous studies, while the influence of two different wind field models was not considered. So far, two wind field models must be investigated.

In addition, only one sample of the wind speed random process was used in the past numerical simulations. Taking into account actual complicated wind field, the multiple dynamic response statistical analysis should be carried out. According to a Japanese standard [23], the response of a single mass system on wind acting 160 times in 10 min was calculated, and the results showed that the interval analysis should be performed at least four times to make the results 90% credible. The multinode system deviations may be larger. Gui-niu [24] analyzed the wind vibration of seven typical high-rise buildings, made statistical analysis of the results, and concluded that the internal forces of the structure, the displacement, and the acceleration responses to the wind on the top are all relatively consistent, verified the correctness and applicability of the method, and provided a reasonable statistical method to assess the wind vibration time history analysis result.

This paper is based on the four-circuit electrical power line. We designed a finite element model of the transmission tower-line system using ANSYS software. The effects of the length of the time history and of the number of samples were investigated. To improve the credibility of the wind vibration response analysis, we selected 600 s sample length of time history and the total number of samples 10 for the further analysis. Based on the engineering practice, we considered 90° wind angle under two wind field models. Then, we carried out statistics and comparative analysis of the wind vibration response of single towers and the transmission tower-line system. Finally, the results obtained with two different wind field models have been compared. This study supplies an advanced statistical analysis of the vibration response of transmission tower-line system.

2. Structural Model

2.1. Project Profile. In this paper, we investigated a 220 kV transmission line of four circuits as the engineering background, adopting the method of strain tower, tangent tower, tangent tower, and strain tower, which spans on 280 m, 653 m, and 259 m. The tangent tower is a four-circuit tower consisted of steel tubes and angel steels, the nominal height of the high tower is 72 m, and its total height is 97.3 m with the root of 22 m; the nominal height of the low tower is 45 m, its total height is 70.3 m, and the root is 11 m. The conductor line is a double split type JLHA2/LB14-630/45, and the upper two ground lines are JLHA2/LB14-95/55. The tower advocate is made of Q345 steel tube, and the other parts are made of Q235 equilateral angle steel. The type and parameters of the lines are listed in Table 1.

2.2. The Finite Element Model. The model of the transmission tower-line system was designed by ANSYS software. We employed Beam 188 unit for simulations; the quality of steel tube and angle steel elements, the nodal plate, auxiliary materials, and fittings is considered by adjusting the density of the material. The elasticity modulus and the Poisson ratio of the steel for Q235 equilateral angle steel and Q345 steel tube were 206 GPa and 0.3, respectively. The tower-line system was built for four circuits. The conductor line of the tower is vertically arranged and consists of four layers. The top one is the ground line, and the remaining layers are four pairs of double split conductors. Each pair of double split conductors and the ground line were simulated with cables. According to the search theory of the conductor line, we used Link 10 to model the line and applied the initial strain for the initial

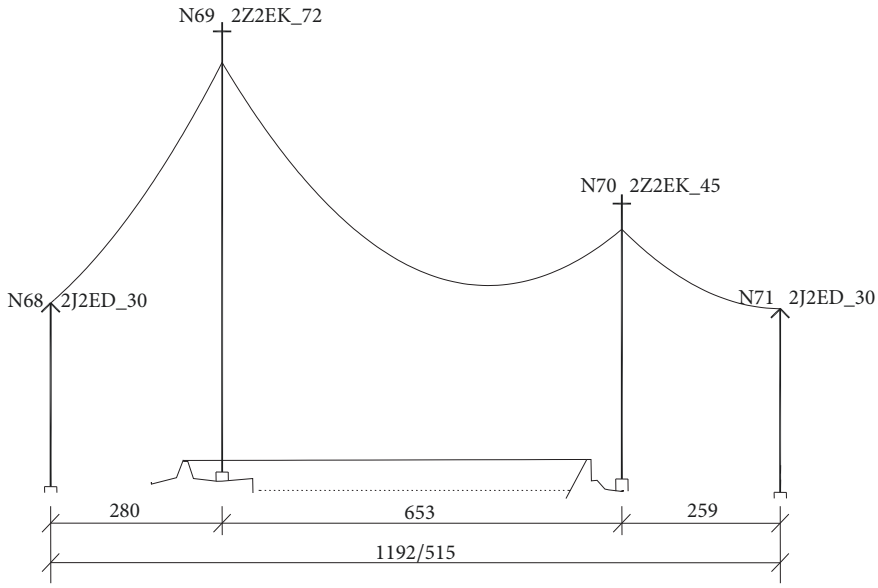

Figure 1: Schematic of the transmission tower-line system crossing a watercourse.

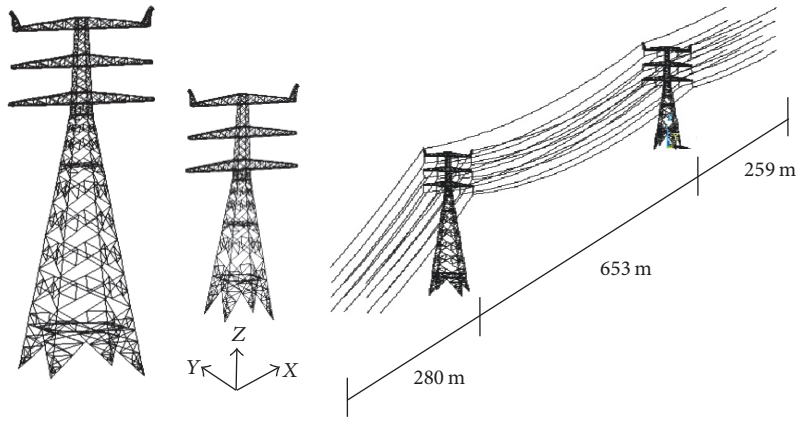

Figure 2: Finite element model of the transmission tower-line system.

stress of the line with the basic length of the element of 20 m. The suspension insulator string was modeled with Link 8. The foot of the tower was fixed with constraints. The stiffness of the tension tower is large, and both ends of the line have fixing constraints. The finite element model of the tower-line system consists of 2450 nodes and 5084 elements. It is shown in Figures 1 and 2.

3. Numerical Simulation of the Wind Speed

3.1. Three-Dimensional Wind Field Parameters. In the wind speed time history curve, the instantaneous wind speed consists of two parts: one is a rather long period of more than 10 min, the mean wind that does not change with time; the other one is the fluctuating wind with the period of a few seconds. The wind speed in the structure can be expressed by the mean wind speed and the fluctuating wind speed. See the following formula:

$$V(x, y, z, t) = \overline{v}(z) + v(x, y, z, t). \quad (1)$$

3.1.1. The Mean Wind. Davenport [25] proposed an exponential function to describe the mean wind speed; it changes with the height. In the wind-resistant design of civil engineering, the exponential function is usually adopted as follows:

$$\frac{\overline{V}(Z)}{\overline{V}(Z_b)} = \left(\frac{Z}{Z_b}\right)^{\alpha}, \quad (2)$$

where $\overline{V}(Z)$ is the mean wind speed at the height of z; $\overline{V}(Z_b)$ is the mean wind speed at the height of z_b; z is the height; Z_b is the standard reference height; α is the ground roughness exponent.

3.1.2. The Fluctuating Wind. The turbulent characteristics of the fluctuating wind within the frequency domain are described by the longitudinal fluctuating wind speed spectrum and the coherence function of the fluctuating wind speed.

The specification in China [26] adopts the Canadian Davenport wind speed spectrum [25]. Davenport obtained more than 90 strong wind records based on different places and heights in the world and established the empirical mathematical expression:

$$S(n) = 4k\overline{V}_{10}^2 \frac{x^2}{n\left(1+x^2\right)^{4/3}},$$
$$x = 1200\frac{n}{\overline{V}_{10}}, \tag{3}$$
$$\overline{V}(z) = \overline{V}_{10} \cdot \left(\frac{z}{10}\right)^{\alpha},$$

where $S(n)$ is the fluctuation wind speed spectrum; n is the frequency; z is the height; $\overline{V}(z)$ is the mean wind speed at the height of z; $\overline{V}_{10}$ is the mean wind speed at the standard height of 10 m; α is the ground roughness exponent; k is the terrain rough factor.

The transmission tower is a high structure, suitable for the use of the Kaimal wind speed spectrum [27] as the target power spectrum to simulate the wind speed. Its mathematical expressions are the following:

$$S(z,n) = 200u_*^2 \frac{f}{n\left(1+50f\right)^{5/3}},$$
$$f = \frac{nz}{\overline{V}(z)},$$
$$\overline{V}(z) = \overline{V}_{10} \cdot \left(\frac{z}{10}\right)^{\alpha}, \tag{4}$$
$$\sigma_v^2 = 6k\overline{V}_{10}^2 = 6u_*^2,$$

where $S(z,n)$ is the fluctuation wind speed spectrum; u_* is the longitudinal friction velocity; σ_v is the root variance of the pulsating wind speed; the rest of the symbolic parameters are the same as in (3).

According to the specification in China [26], the three-dimensional frequency-independent spatial coherence function was adopted by Shiotani and Arai [28]. Its expression is as follows:

$$\underset{i,j}{\mathrm{Coh}}(r) = \exp\left(-\sqrt{\sum_r \frac{\left(r_i - r_j\right)^2}{L_r^2}}\right), \tag{5}$$

where $\mathrm{Coh}_{i,j}(r)$ is the square root of the coherent function; $r = x, y, z$ are the coordinates; $L_x = 50$, $L_y = 50$, $L_z = 60$.

The coherence function proposed by Davenport [25] is related to the frequency, and its expression is

$$\underset{i,j}{\mathrm{Coh}}(r,n) = \exp\left(\frac{-2n\sqrt{\sum_r C_r^2\left(r_i - r_j\right)^2}}{\left(\overline{V}(z_i) + \overline{V}\left(z_j\right)\right)}\right), \tag{6}$$

where $\mathrm{Coh}_{i,j}(r,n)$ is the square root of the coherent function; n is the frequency; $r = x, y, z$ are the coordinates; $\overline{V}(z_i)$, $\overline{V}(z_j)$ are the mean wind speed at the heights of z_i and z_j; C_x, C_y, C_z are the attenuation coefficient, $C_x = 16$, $C_y = 8$, $C_z = 10$.

3.1.3. Method of Numerical Simulation of the Fluctuating Wind Speed. Many researchers in China and abroad observed and studied the fluctuating wind, and it is generally believed that the fluctuating wind can be approximated as a stationary random process with a zero mean value. The simulation method of the stationary random process is divided into two kinds: linear filtration and harmonic synthesis. In recent years, the Autoregressive (AR) model of the linear filtering method is widely used in studies of random vibrations and the time domain analysis. It possesses a small amount of calculations and fast. After the linear filtering, the white noise random process (zero mean value) becomes a stationary random process with the characteristic spectrum. In this paper, the numerical simulation of the fluctuating wind speed was carried out by the Autoregressive model of the linear filtering method (AR [29]).

The AR model of M points associated with the fluctuating wind $V(X,Y,Z,t)$ is expressed as follows:

$$V(X,Y,Z,t) = -\sum_{k=1}^{p} \psi_k V(X,Y,Z,t-k\Delta t) + N(t), \tag{7}$$

where $X = [x_1, x_2, \ldots, x_M]^T$, $Y = [y_1, y_2, \ldots, y_M]^T$, $Z = [z_1, z_2, \ldots, z_M]^T$, (x_i, y_i, z_i) are the coordinates of number i point, $i = 1, 2, \ldots, M$; p is the order number of AR model; Δt is the time step; ψ_k is $M \times M$ matrix, the Autoregressive coefficient matrix of AR model; $k = 1, 2, \ldots, p$; $N(t)$ is the independent random process vector.

3.2. Simulation of the Wind Speed Time History. The main parameters of the wind speed simulation are shown in Table 2, according to the specification in China [26] and the engineering practice. The specification in China states that the fluctuating wind field is composed of Davenport wind speed spectrum and Shiotani coherence function. Therefore, this paper considers Davenport wind speed spectrum and Shiotani coherence function as the wind field 1, but Davenport wind speed spectrum does not change with altitude, while Kaimal wind speed spectrum changes with altitude. The transmission tower is a high structure, suitable for the use of the Kaimal wind speed spectrum as the target power spectrum to simulate the wind speed. In addition, Shiotani coherence function does not take into account the frequency, However, Davenport coherence function is related to the frequency. Therefore, this paper considers the Kaimal wind speed spectrum and Davenport coherence function as the wind field 2.

Due to the large node of the transmission tower, we simplified the simulation area in this paper. Figure 3 shows the subsection schematic of single towers and lines. We used the wind speed simulation at a centre point as the representative of each area. In each area, the wind speed time history at all nodes is the same as the wind speed time history of the representative point. Using MATLAB software to initiate the fluctuating wind speed time history simulation

Table 2: The main parameters of wind speed simulation.

Parameters	Values
Surface roughness class	A type ($\alpha = 0.12$, $k = 0.00129$)
Mean wind profile	Exponential function
$\overline{V}_{10}$	35 m/s
Fluctuation wind speed spectrum	Davenport/Kaimal
Coherence function	Shiotani/Davenport
Simulation method	The Autoregressive model of linear filtering method (AR) ($P = 4$)
Length of time history	100 s, 200 s, 600 s, 1000 s, 2000 s
Number of samples	1, 3, 5, 8, 10
Time step	0.1 s
Frequency range	The initial frequency is 0.01 Hz and the end frequency is 10 Hz

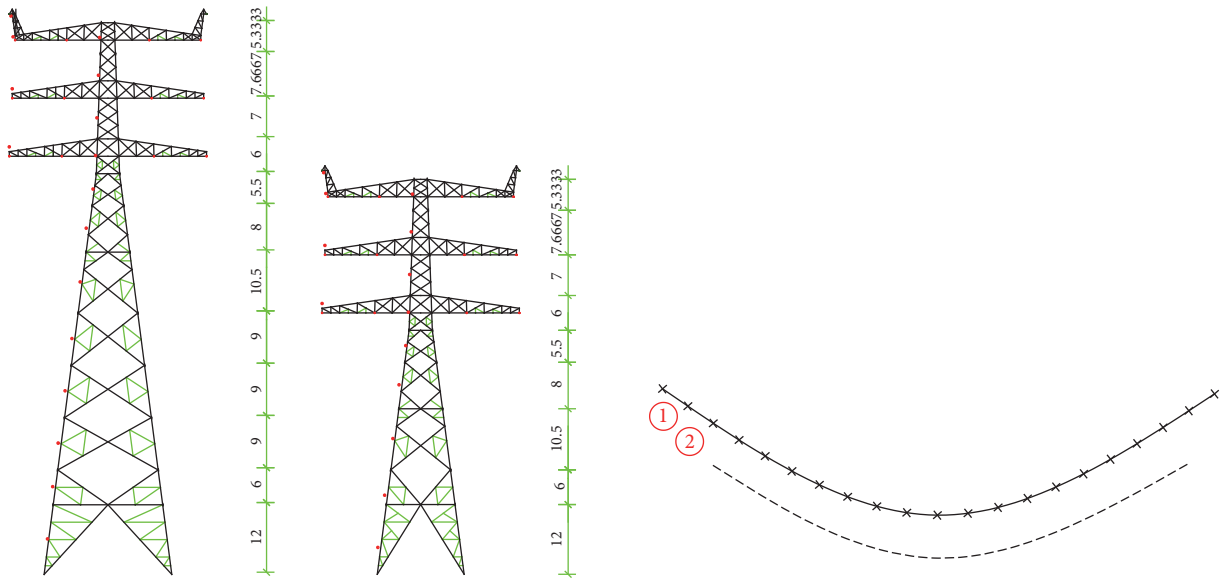

Figure 3: Subsection schematic of single towers and lines.

program, we simulated the wind speed for the single towers and the lines, respectively.

We used AR model of the linear filtering method (AR [29]) to simulate the wind speed time history at 90° wind angle. Figure 4 shows the simulation results of the fluctuating wind speed time history for the transmission tower-line system at 61.05 m, sample 5, under the influence of wind fields 1 and 2. Figure 5 shows the comparison of the fluctuating wind speed spectrum with the target spectrum at 61.05 m, sample 5, under wind fields 1 and 2.

It can be seen from Figure 5 that the spectral line trend of the simulated spectrum is consistent with that of the target spectrum. Using the Autoregressive model of the linear filtering method (AR model) to simulate the wind field, we achieve good accuracy. The simulation results of the wind speed time history show that the fluctuating wind under Davenport wind speed spectrum possesses more broad fluctuation range.

3.3. Calculation of the Wind Load Time History. According to the manual description in China [30], the wind load on the transmission tower can be expressed as follows:

$$W_t = kA_p \frac{V^2}{1.6}, \tag{8}$$

where W_t is the wind load for transmission tower; k is the wind load shape coefficient; A_p is the wind area of the element in the transmission tower; V is the wind speed.

When the wind load is applied to the towers, after working out each section of the wind load, the load values were distributed into four nodes in this section of the whole body of the tower to calculate the internal forces of the structure.

The wind load of the line can be expressed as follows:

$$W_x = \alpha \cdot \beta_c \cdot \mu_s \cdot \mu_z \cdot w_0 \cdot d \cdot L_h \cdot \sin^2\theta, \tag{9}$$

where W_x is the standard value of horizontal wind load for vertical line action; α is the uneven factor of the wind speed;

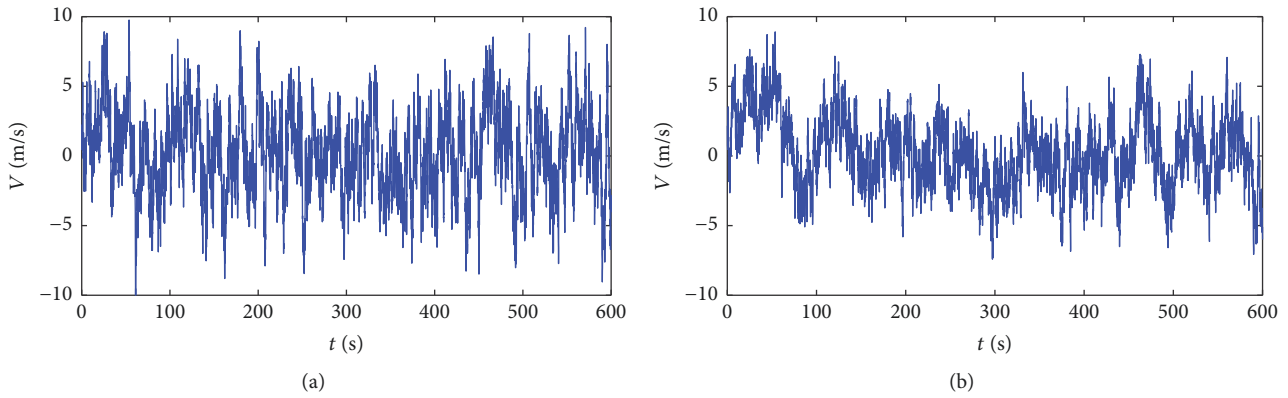

Figure 4: The fluctuating wind speed time history under wind fields 1 and 2.

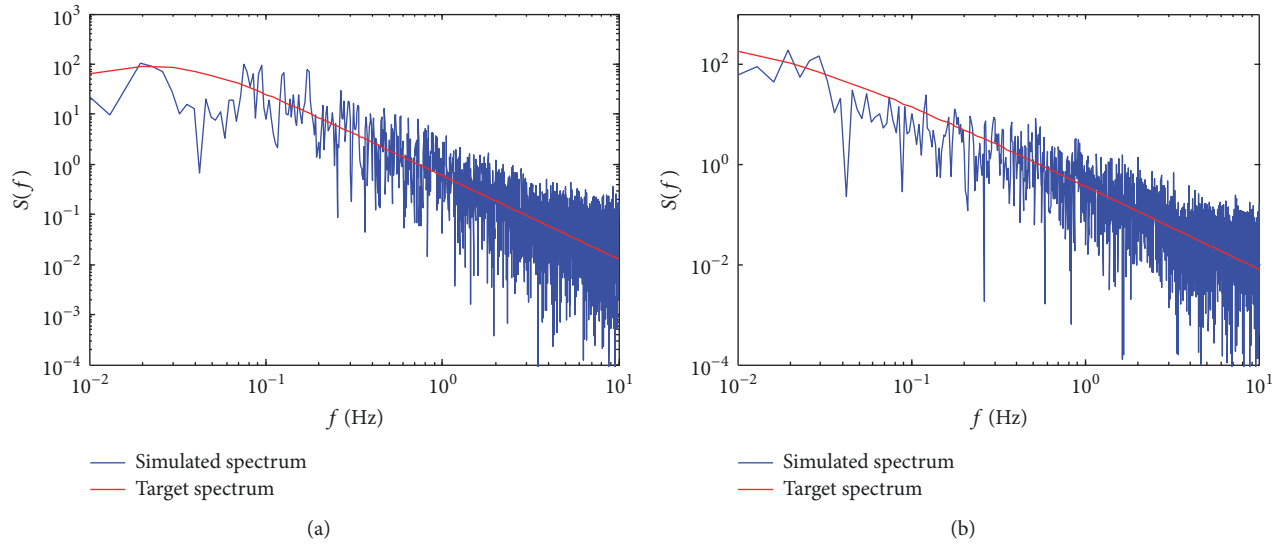

Figure 5: Comparison of the pulsating wind speed spectrum with the target spectrum under wind fields 1 and 2.

β_c is the wind load adjustment coefficient of the line; μ_s is the wind load shape coefficient of the line diameter < 17 mm or ice cover (no matter the diameter of the wire), $\mu_s = 1.2$, the wire diameter ⩾ 17 mm, and the wire is not ice covered, $\mu_s = 1.1$; μ_z is the wind pressure height coefficient; d is the diameter of the line or the mean outer diameter of the line under ice cover (for bundled conductor, the outer diameter of the subconductor). L_h is horizontal span; θ is the angle between the wind and the line; W_0 is the wind pressure, $W_0 = V^2/1600$.

When the wind load is applied to the lines, it is also applied to nodes of the sections.

4. Statistical Analysis of the Wind-Induced Dynamic Response

Figure 6 shows the location map of the maximum displacement nodes and the maximum axial force elements.

4.1. Total Length and Total Number of Samples Selection. In this paper, the total time history length and a total number of samples are selected for the high tower (without the load of the lines). The length is 100 s, 200 s, 600 s, 1000 s, and 2000 s; the total number of samples is 1, 3, 5, 8, 10. To analyze the results of the average dynamic response, we removed the first 10 s of the unstable stage of structural vibration. The statistical comparison and analysis results of the calculation of the Ux displacement (the displacement along the wind direction) on high tower top node 35# are presented in Tables 3, 4, and 5.

It can be seen from Table 3 that the extreme displacement value increases gradually with the increase of the sample length; the reason of this phenomenon is that there will be such result in the dynamic analysis, and the numerical is very big but the frequency is very low, relating to the sample length. With an increase in the sample length, the error of this method also increases as the statistical result of dynamic response. It can be concluded from Table 3 that the extreme

Table 3: The average of extremum Ux displacement on tower top node 35# (mm).

		The length of samples (s)				
		100	200	600	1000	2000
The total number of samples	1	170.52	176.07	172.02	176.38	185.61
	3	167.29	179.30	172.84	177.68	181.66
	5	168.59	176.76	171.85	176.58	185.29
	8	169.94	173.83	170.77	180.29	184.28
	10	169.77	173.44	171.71	179.58	183.38

Table 4: The average of mean Ux displacement on tower top node 35# (mm).

		The length of samples (s)				
		100	200	600	1000	2000
The total number of samples	1	124.27	126.19	123.76	123.11	124.46
	3	121.85	124.86	123.23	124.78	124.63
	5	124.37	124.21	123.78	124.53	124.95
	8	124.73	123.41	123.27	124.67	125.00
	10	124.44	123.63	123.45	124.59	124.92

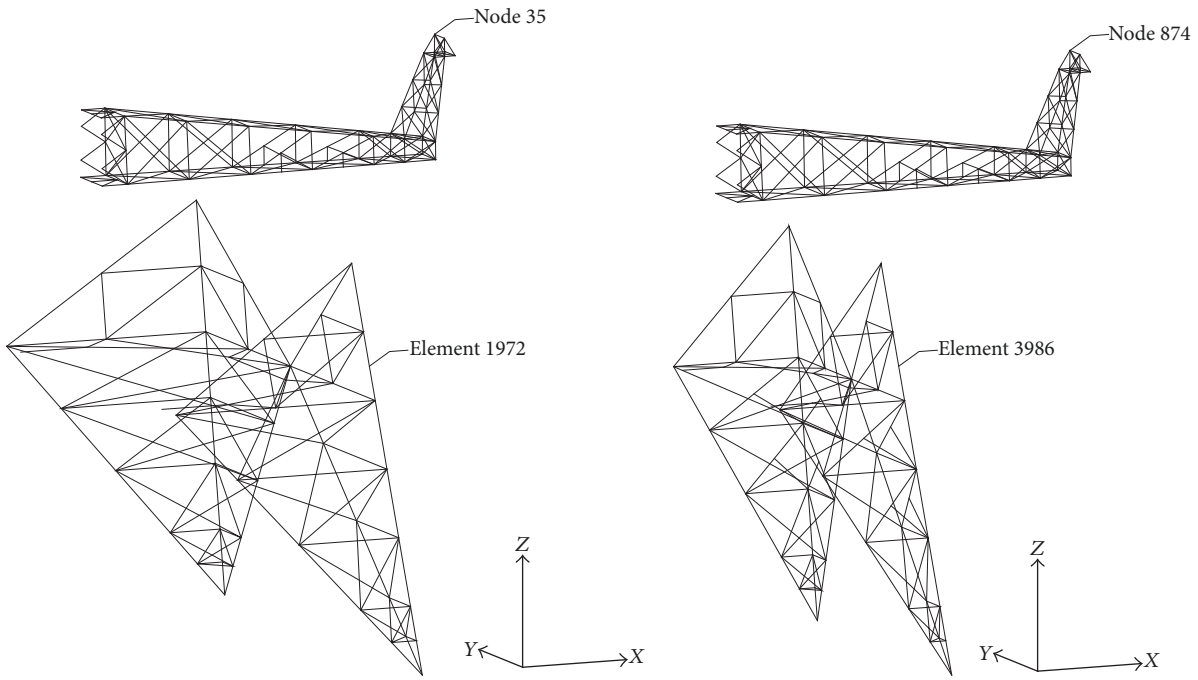

(a) High tower (b) Low tower

Figure 6: The location map of the maximum displacement nodes and the maximum axial force elements.

displacement value is not consistent with one sample. The relative error of the statistical results for the number of more than one sample is no more than 2%, and the deviation is small.

The relative error of the mean value of the displacement response (Table 4) is no more than 3%; it does not change with the sample length and the number of samples. The average wind that is equivalent to static forces is the main factor that causes the average result; thus, the statistical results of the time history are calculated on average.

From Table 5, it can be seen that the root variance of the displacement response tends to a certain fixed value with an increase in the sample length and the number of samples. This value is about 14.50 mm. The effect of sample length variation is small, and the relative error is about 8%, which can be reduced by an increase in the number of samples.

Table 5: The average of variance Ux displacement on tower top node 35# (mm).

		The length of samples (s)				
		100	200	600	1000	2000
The total number of samples	1	14.54	14.06	13.60	15.48	14.14
	3	13.88	15.03	13.65	14.83	14.23
	5	14.41	14.97	14.04	14.64	14.35
	8	14.89	14.61	14.33	14.76	14.47
	10	14.71	14.50	14.32	14.73	14.51

Table 6: Statistics of 10 samples parameters of the single high tower top node 35# Ux displacement time history under wind field 1 (m).

Displacement	Mean	SD	Skewness	Kurtosis	Minimum	Maximum
Sample 1	0.35442	0.06831	0.13752	0.09248	0.12564	0.62239
Sample 2	0.35890	0.07097	0.05107	−0.15181	0.11660	0.57983
Sample 3	0.35444	0.06559	0.05681	0.34004	0.12688	0.63887
Sample 4	0.35050	0.06803	−0.02753	0.13739	0.08682	0.59494
Sample 5	0.35621	0.06778	−0.13817	−0.06441	0.07765	0.58402
Sample 6	0.34745	0.06941	0.17547	0.12119	0.11916	0.61964
Sample 7	0.35154	0.07096	0.05388	0.09499	0.10151	0.58926
Sample 8	0.35595	0.06740	0.02192	0.19480	0.10866	0.63173
Sample 9	0.35450	0.06794	0.01347	−0.19614	0.14479	0.56227
Sample 10	0.35138	0.06998	−0.03027	−0.12573	0.12174	0.5984

To sum up, we resume that high accuracy of the calculation results of the wind-induced nonlinear dynamic response statistics may be provided by the length of samples of 600 s and the total number of samples of 10. The time step was 0.1 s, excluding the initial 10 s of the unstable stage in structural vibration, and the total number of statistical points was 59,000.

4.2. Dynamic Response Statistical Analysis. Using ANSYS and Origin software, we analyzed the nonlinear dynamic response of single towers and the tower-line system for the selected 600 s length 10 samples under two kinds of the wind field. Figures 7–14 show the time history curves and the frequency histograms of the single tower and tower in the tower-line system under wind fields 1 and 2.

The frequency histograms show that the frequency distribution of displacement and axial force statistical results possess Gaussian distribution (thin lines are the Gaussian curve fittings by Origin).

Tables 6–21 present statistics of 10 samples parameters of single towers and towers in the system under two kinds of the wind field.

In Tables 6–21, one may see the statistical description of the samples from the central tendency, the dispersion degree, the Skewness, and Kurtosis. The Skewness and Kurtosis describe particular characteristics of an individual sample. Skewness characterizes the distribution of symmetry. Kurtosis is a measure of the degree of Kurtosis of a set of data. As can be seen from Tables 6–21, the values of Skewness and Kurtosis are basically around 0 that is in accordance with the Gaussian distribution.

We used three statistical methods in this paper [31]. Method 1, the maximum average: the extreme value in the analysis of the wind vibration is not most representative, but sometimes it cannot be ignored. Considering the maximum average results as a statistical result is relatively conservative. Method 2, "3 σ rule": we add three times root variance to the mean of samples. And then we calculate the average of the sum: in the simulation, the wind speed is assumed to be a stationary Gaussian random process; the time history analysis results basically have normal distribution, also following "3 σ rule" of statistical analysis. Method 3, the root mean squares average (RMS): because the average of the fluctuating wind is near zero, the wind-induced dynamic response of displacement and internal force response of root mean square (RMS) value is approximately equal to the average, so it relates to the response caused by the average wind.

The dynamic response displacements and axial force values of single towers and the transmission tower-line system were obtained for the sample length of 600 s and 10 samples by the three statistical methods mentioned above, and the results are listed in Tables 22–25.

5. Conclusion

Based on the numerical simulation method, the dynamic response of the transmission tower-line system is obtained within the sample length of 600 s for 10 samples. The conclusions are the following:

(1) The Autoregressive model of linear filtering method (AR model) provides good accuracy of the wind field simulation. The simulation results of the wind speed time history show that the fluctuating wind under Davenport wind speed spectrum has broad fluctuation range. The wind speed fluctuation range simulated under Kaimal wind speed spectrum is less broad.

Table 7: Statistics of 10 samples parameters of the single high tower element 1972# axial force time history under wind field 1 (N).

Axial force	Mean	SD	Skewness	Kurtosis	Minimum	maximum
Sample 1	−2949190	225007	−0.17856	0.07085	−3822520	−2119440
Sample 2	−2950810	232705	−0.03571	−0.15095	−3660450	−2131130
Sample 3	−2937700	219395	−0.07871	0.40531	−3985950	−2135060
Sample 4	−2940790	225055	0.03573	0.15023	−3730720	−2032810
Sample 5	−2941240	225111	0.14216	0.02959	−3762320	−1956890
Sample 6	−2931170	232844	−0.20734	0.12401	−3910300	−2142180
Sample 7	−2935120	232508	−0.04941	0.05375	−3698390	−2099490
Sample 8	−2936460	227044	0.00731	0.03378	−3816710	−2145960
Sample 9	−2927360	228612	−0.01472	−0.13648	−3705960	−2211190
Sample 10	−2938370	230554	0.0376	−0.13684	−3739450	−2212520

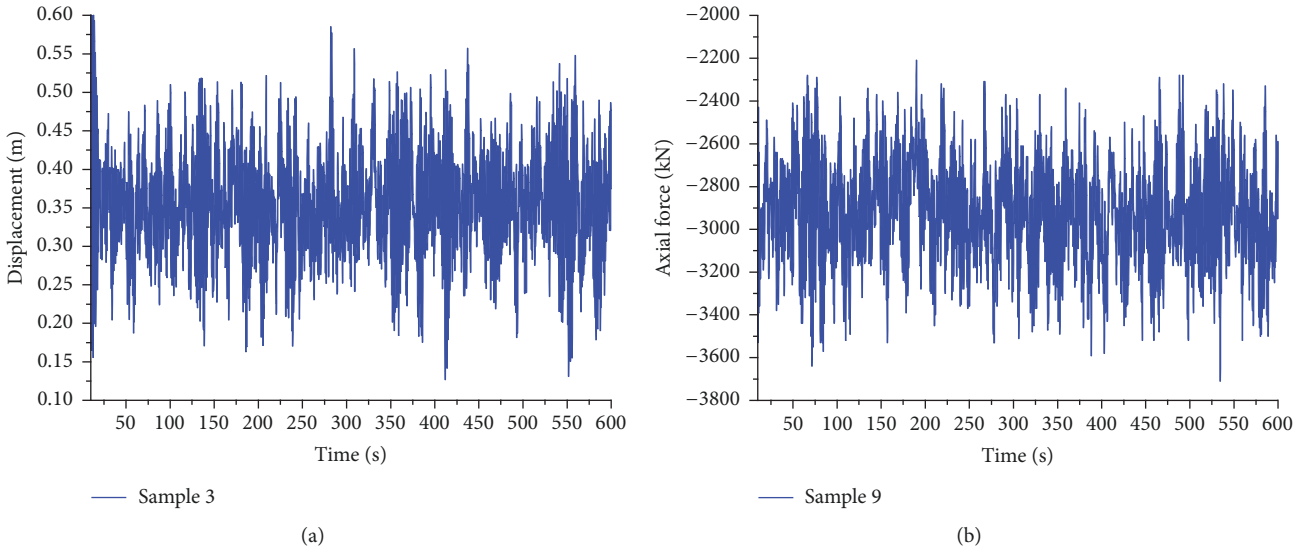

Figure 7: Time history curve of single high tower under wind field 1.

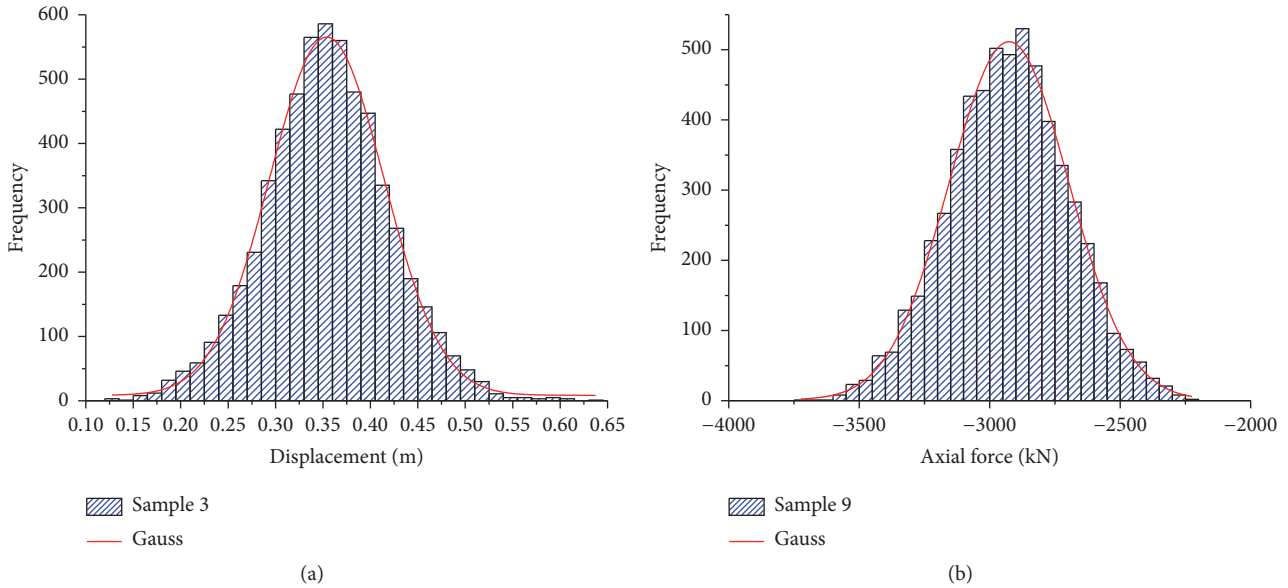

Figure 8: Frequency histogram of single high tower under wind field 1.

Table 8: Statistics of 10 samples parameters of the single high tower top node 35# Ux displacement time history under wind field 2 (m).

Displacement	Mean	SD	Skewness	Kurtosis	Minimum	Maximum
Sample 1	0.35656	0.03693	−0.18703	−0.03583	0.21504	0.47104
Sample 2	0.35073	0.03515	0.23975	0.21275	0.25089	0.49667
Sample 3	0.34378	0.03559	−0.06313	−0.01272	0.21787	0.45803
Sample 4	0.35171	0.03376	−0.04804	−0.07481	0.23818	0.47092
Sample 5	0.35240	0.03495	−0.15822	0.04742	0.22354	0.46427
Sample 6	0.35231	0.03791	−0.19994	0.46160	0.19914	0.46968
Sample 7	0.34313	0.03985	−0.03358	−0.19496	0.19995	0.47154
Sample 8	0.34723	0.03761	−0.02709	−0.04106	0.22602	0.46813
Sample 9	0.34644	0.03561	−0.13752	−0.25035	0.21269	0.45174
Sample 10	0.35075	0.03550	−0.11431	0.00106	0.21375	0.49495

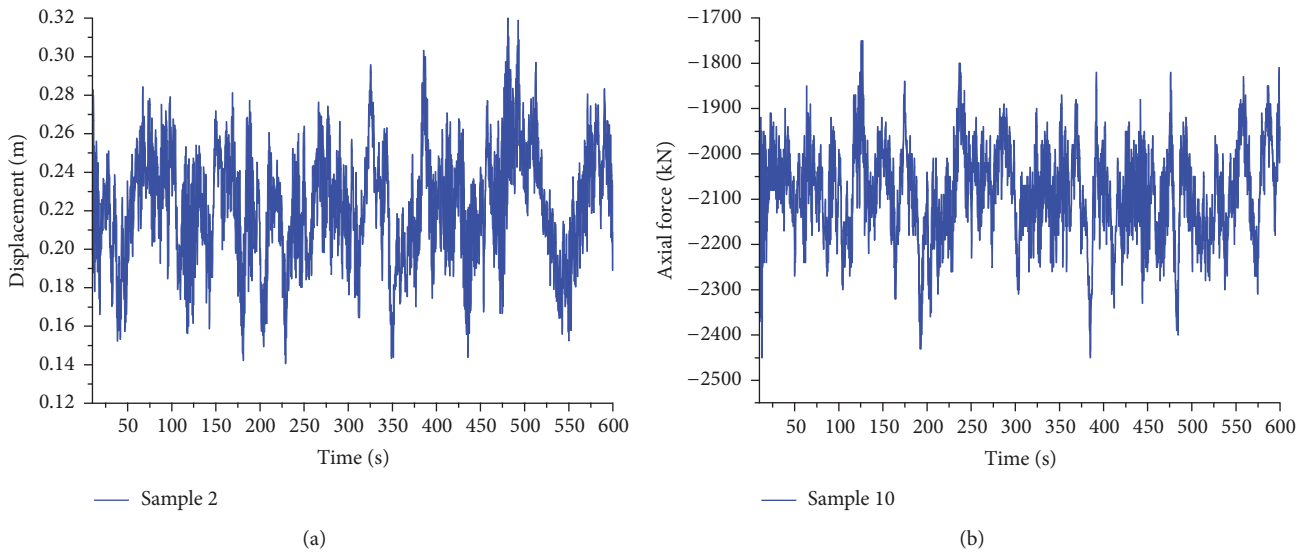

Figure 9: Time history curve of single low tower under wind field 2.

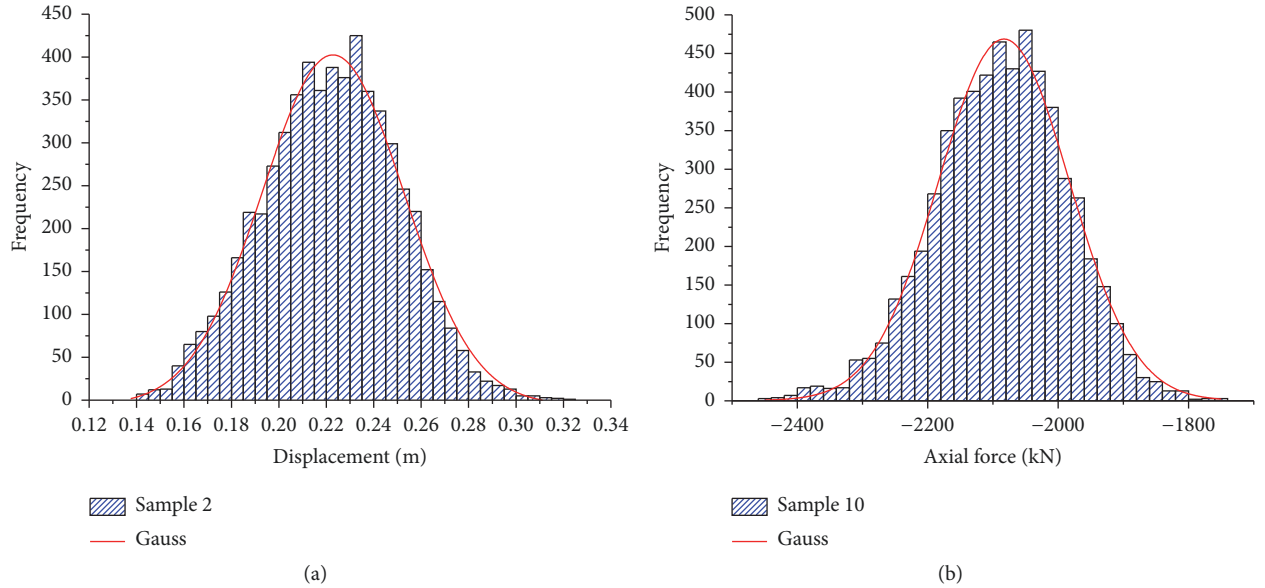

Figure 10: Frequency histogram of single low tower under wind field 2.

Table 9: Statistics of 10 samples parameters of the single high tower element 1972# axial force time history under wind field 2 (N).

Axial force	Mean	SD	Skewness	Kurtosis	Minimum	maximum
Sample 1	−2948080	140919	0.17295	−0.17540	−3370600	−2444340
Sample 2	−2935270	132886	−0.26298	0.19441	−3477780	−2534960
Sample 3	−2905090	134097	0.16187	0.05996	−3339770	−2400450
Sample 4	−2930700	127225	0.02708	−0.10905	−3376020	−2549530
Sample 5	−2942440	130176	0.15989	−0.01083	−3319490	−2430920
Sample 6	−2923830	143796	0.16689	0.32566	−3368890	−2332000
Sample 7	−2902400	153641	0.08227	−0.21682	−3376560	−2331160
Sample 8	−2921840	142735	−0.04108	−0.19449	−3413370	−2492820
Sample 9	−2907490	132675	0.13648	−0.30934	−3263360	−2526720
Sample 10	−2932580	134586	0.1526	−0.14411	−3447680	−2437930

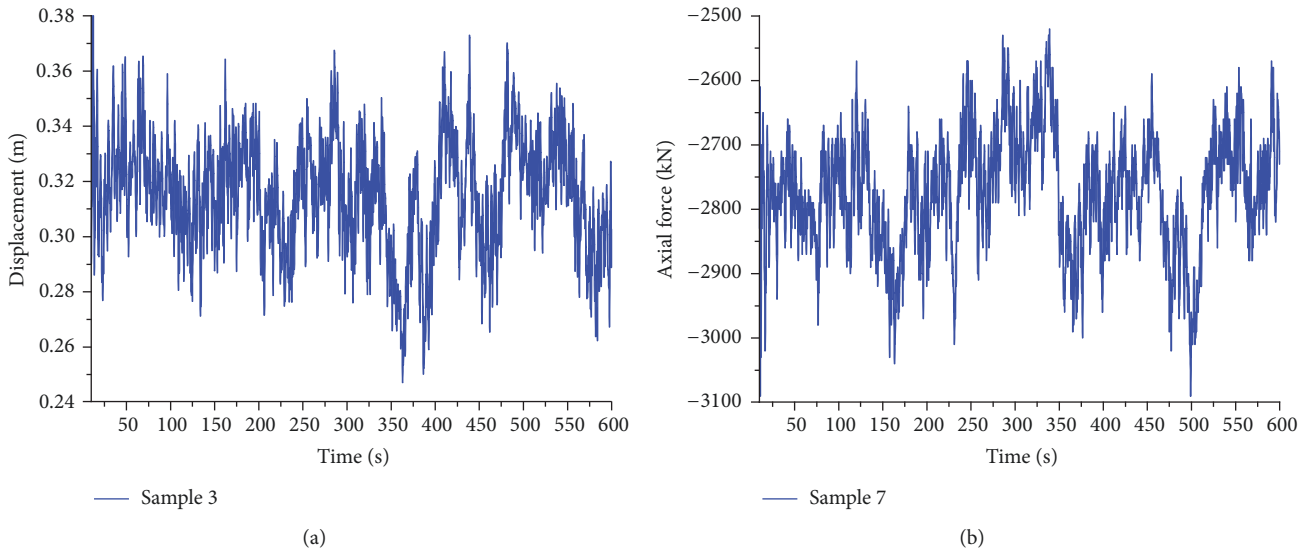

Figure 11: Time history curve of high tower in the tower-line system under wind field 2.

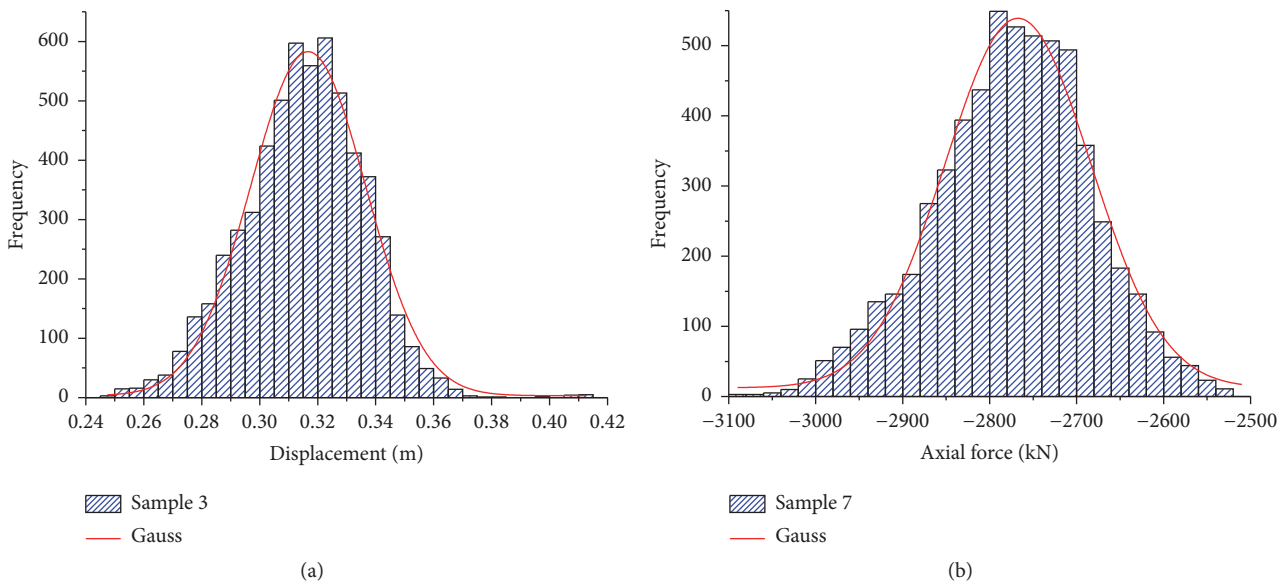

Figure 12: Frequency histogram of high tower in the tower-line system under wind field 2.

Table 10: Statistics of 10 samples parameters of the single low tower top node 874# Ux displacement time history under wind field 1 (m).

Displacement	Mean	SD	Skewness	Kurtosis	Minimum	Maximum
Sample 1	0.22218	0.04530	−0.02671	0.38976	0.02268	0.42222
Sample 2	0.22022	0.04435	−0.1314	0.18416	0.03907	0.3918
Sample 3	0.22132	0.04658	−0.0305	0.02998	0.06550	0.38712
Sample 4	0.21970	0.04688	−0.01637	−0.01960	0.04685	0.38675
Sample 5	0.22132	0.04325	−0.03241	−0.19524	0.07749	0.35659
Sample 6	0.21745	0.04478	0.05446	−0.00820	0.06996	0.3807
Sample 7	0.22377	0.04309	0.0077	−0.25533	0.08035	0.38412
Sample 8	0.22365	0.04780	0.1368	0.17935	0.05807	0.40093
Sample 9	0.22044	0.04361	0.0464	0.16881	0.06084	0.39196
Sample 10	0.21944	0.04352	0.00647	−0.02461	0.05496	0.37344

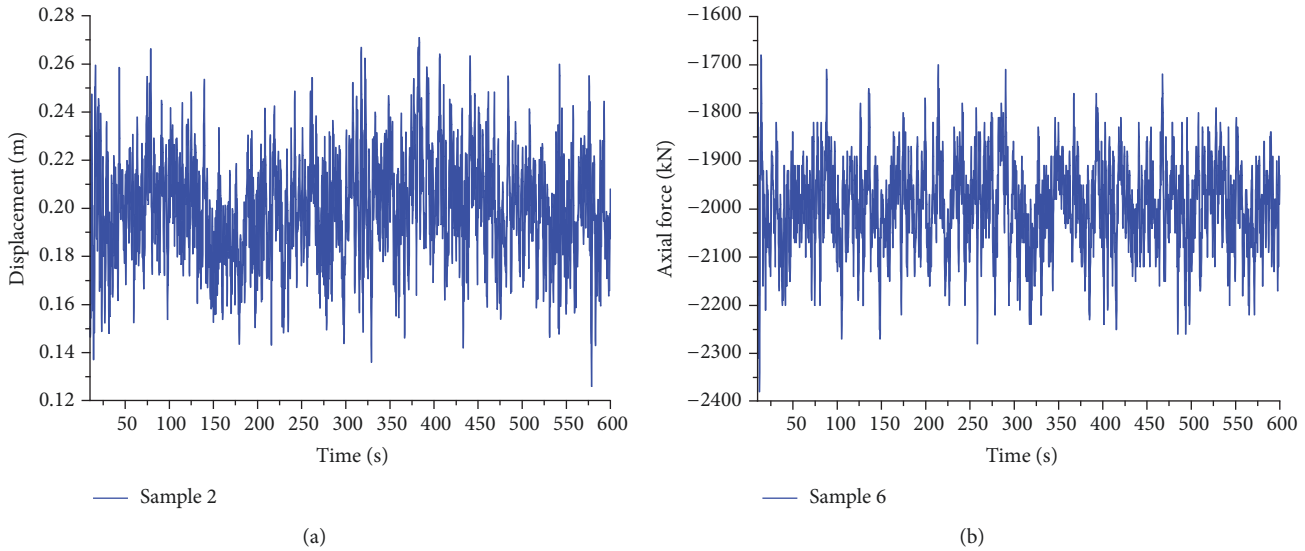

Figure 13: Time history curve of low tower in the tower-line system under wind field 1.

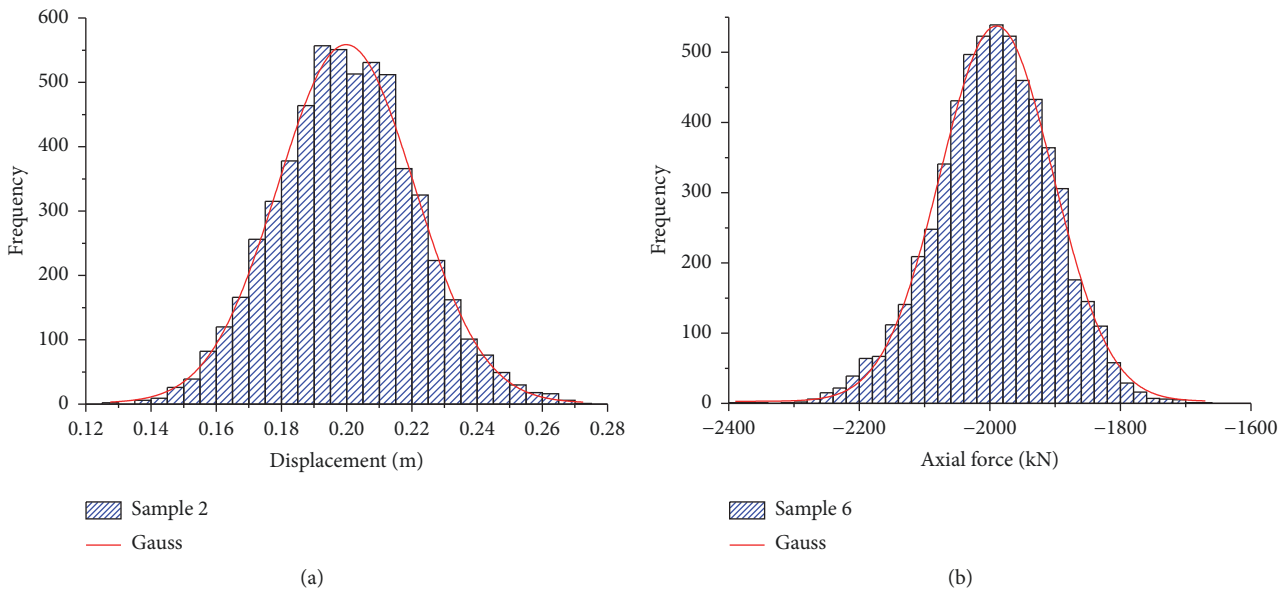

Figure 14: Frequency histogram of low tower in the tower-line system under wind field 1.

Table 11: Statistics of 10 samples parameters of the single low tower element 3986# axial force time history under wind field 1 (N).

Axial force	Mean	SD	Skewness	Kurtosis	Minimum	maximum
Sample 1	−2082860	169524	0.01765	0.34298	−2832540	−1319350
Sample 2	−2073850	162592	0.13724	0.13390	−2656770	−1448890
Sample 3	−2077750	174300	0.05555	−0.04310	−2655310	−1522670
Sample 4	−2068890	173793	0.02291	−0.07825	−2666350	−1421670
Sample 5	−2078850	161427	−0.00686	−0.24323	−2584010	−1584550
Sample 6	−2060190	166659	−0.0369	−0.03360	−2654160	−1465200
Sample 7	−2088820	158783	−0.00452	−0.17713	−2714900	−1553110
Sample 8	−2083710	177654	−0.19925	0.19016	−2777500	−1513340
Sample 9	−2075190	159751	−0.02932	0.13758	−2664530	−1492870
Sample 10	−2069550	160157	−0.02257	−0.00476	−2633630	−1525840

Table 12: Statistics of 10 samples parameters of the single low tower top node 874# Ux displacement time history under wind field 2 (m).

Displacement	Mean	SD	Skewness	Kurtosis	Minimum	Maximum
Sample 1	0.22514	0.02572	−0.03497	0.35147	0.10754	0.31219
Sample 2	0.22209	0.02837	−0.02827	−0.22073	0.14054	0.32388
Sample 3	0.22374	0.02627	0.01650	−0.23694	0.12845	0.31262
Sample 4	0.21937	0.02918	0.09423	−0.10346	0.12755	0.31399
Sample 5	0.22691	0.02537	0.17305	0.16969	0.11514	0.31096
Sample 6	0.21709	0.02526	−0.02530	−0.15620	0.12656	0.30634
Sample 7	0.22686	0.02407	−0.09220	0.15697	0.13991	0.31507
Sample 8	0.21504	0.02781	0.01384	−0.01940	0.12086	0.30812
Sample 9	0.21722	0.02517	−0.11976	0.66410	0.12086	0.32400
Sample 10	0.22322	0.02428	0.09103	−0.01395	0.13545	0.30322

Table 13: Statistics of 10 samples parameters of the single low tower element 3986# axial force time history under wind field 2 (N).

Axial force	Mean	SD	Skewness	Kurtosis	Minimum	maximum
Sample 1	−2094690	107707	0.0077	0.22676	−2452950	−1616830
Sample 2	−2082530	118333	0.02739	−0.24416	−2500100	−1732870
Sample 3	−2090200	110671	−0.000196	−0.25047	−2453230	−1702140
Sample 4	−2068760	122979	−0.09519	−0.16871	−2454330	−1708950
Sample 5	−2101960	108367	−0.20278	0.15694	−2453410	−1628760
Sample 6	−2059300	104250	0.06863	−0.17650	−2425230	−1687330
Sample 7	−2104580	101206	0.06531	0.18746	−2500850	−1750660
Sample 8	−2049980	117069	−0.01751	−0.04761	−2429990	−1668020
Sample 9	−2060060	106047	0.23684	0.86047	−2494290	−1629370
Sample 10	−2087080	101083	−0.17578	0.14326	−2451000	−1745540

Table 14: Statistics of 10 samples parameters of high tower in the system top node 35# Ux displacement time history under wind field 1 (m).

Displacement	Mean	SD	Skewness	Kurtosis	Minimum	Maximum
Sample 1	0.32330	0.02974	0.10779	0.18315	0.22458	0.44661
Sample 2	0.31841	0.03038	−0.02766	−0.00132	0.21733	0.43928
Sample 3	0.31864	0.02934	0.08242	−0.11575	0.22185	0.4174
Sample 4	0.32026	0.03065	−0.00738	0.08926	0.20795	0.42238
Sample 5	0.32299	0.03063	0.04103	0.20988	0.18418	0.44216
Sample 6	0.32308	0.02990	−0.0116	0.30768	0.21552	0.43896
Sample 7	0.32486	0.03049	0.03309	0.00446	0.22536	0.43633
Sample 8	0.32136	0.03042	0.03473	0.10439	0.20734	0.44905
Sample 9	0.32192	0.03045	−0.10315	0.08275	0.21565	0.41596
Sample 10	0.32186	0.03094	0.13139	−0.14000	0.21494	0.43481

Table 15: Statistics of 10 samples parameters of high tower in the system element 1972# axial force time history under wind field 1 (N).

Axial force	Mean	SD	Skewness	Kurtosis	Minimum	maximum
Sample 1	−2764420	117829	−0.08952	−0.06287	−3153370	−2368250
Sample 2	−2745900	115359	0.0534	−0.04482	−3155580	−2354910
Sample 3	−2751510	114232	−0.05331	−0.00765	−3169110	−2340380
Sample 4	−2756110	120891	−0.04072	−0.08704	−3177180	−2372540
Sample 5	−2766420	119284	−0.03748	0.11486	−3245510	−2305030
Sample 6	−2767990	116249	−0.01359	0.18738	−3171830	−2374290
Sample 7	−2774830	119638	0.11258	0.01836	−3141770	−2336580
Sample 8	−2761040	118749	0.0004	−0.01720	−3176570	−2347060
Sample 9	−2762820	120316	0.05717	0.05883	−3188790	−2362880
Sample 10	−2766160	121813	−0.056	−0.19360	−3139350	−2348950

Table 16: Statistics of 10 samples parameters of high tower in the system top node 35# Ux displacement time history under wind field 2 (m).

Displacement	Mean	SD	Skewness	Kurtosis	Minimum	Maximum
Sample 1	0.32390	0.01979	0.02170	−0.10203	0.26349	0.40088
Sample 2	0.31469	0.02212	−0.20609	0.23266	0.23122	0.37960
Sample 3	0.31516	0.02067	−0.08654	0.50949	0.24704	0.41275
Sample 4	0.31720	0.02374	0.20045	−0.21313	0.23982	0.40715
Sample 5	0.32499	0.02618	0.34043	0.14454	0.25832	0.41941
Sample 6	0.32549	0.02616	−0.10295	0.17649	0.23848	0.41391
Sample 7	0.32417	0.02269	0.33877	0.12758	0.25590	0.41618
Sample 8	0.31876	0.02523	0.07881	0.05582	0.24046	0.42604
Sample 9	0.31902	0.02232	0.10203	0.06224	0.25438	0.40586
Sample 10	0.32502	0.02393	−0.08207	−0.09111	0.24802	0.41339

Table 17: Statistics of 10 samples parameters of high tower in the system element 1972# axial force time history under wind field 2 (N).

Axial force	Mean	SD	Skewness	Kurtosis	Minimum	maximum
Sample 1	−2766730	80424	0.09442	0.04115	−3040150	−2484060
Sample 2	−2729260	89952	0.36791	0.23231	−3025500	−2366020
Sample 3	−2734140	85454	0.1637	0.15528	−3136020	−2459260
Sample 4	−2740050	102842	−0.26335	−0.33218	−3106210	−2456440
Sample 5	−2773030	109547	−0.38259	0.24823	−3155320	−2454760
Sample 6	−2777580	109056	−0.07278	0.36029	−3137000	−2430630
Sample 7	−2774270	90187	−0.21247	0.00087	−3089440	−2480530
Sample 8	−2746430	109665	−0.08952	0.00632	−3094720	−2375430
Sample 9	−2750570	94028	−0.07622	−0.06608	−3214130	−2479610
Sample 10	−2779340	98622	0.21257	0.12578	−3099170	−2434880

Table 18: Statistics of 10 samples parameters of low tower in the system top node 874# Ux displacement time history under wind field 1 (m).

Displacement	Mean	SD	Skewness	Kurtosis	Minimum	Maximum
Sample 1	0.20172	0.02069	0.17222	0.23026	0.13554	0.30662
Sample 2	0.20006	0.02114	0.08235	0.00699	0.12600	0.27096
Sample 3	0.20069	0.02073	0.06948	0.10717	0.12750	0.2815
Sample 4	0.19951	0.01945	0.1794	0.27326	0.12948	0.28295
Sample 5	0.20105	0.02043	0.05912	0.05919	0.13795	0.27355
Sample 6	0.20208	0.02008	0.13388	0.04497	0.13019	0.26971
Sample 7	0.20135	0.02076	0.14814	0.25605	0.13445	0.29724
Sample 8	0.20067	0.01950	0.12126	0.02237	0.12363	0.27096
Sample 9	0.20280	0.01959	0.16538	0.24519	0.13675	0.29595
Sample 10	0.19928	0.02025	0.0133	0.05149	0.11540	0.27521

Table 19: Statistics of 10 samples parameters of low tower in the system element 3986# axial force time history under wind field 1 (N).

Axial force	Mean	SD	Skewness	Kurtosis	Minimum	maximum
Sample 1	−1989210	91975	−0.23888	0.53071	−2486860	−1723230
Sample 2	−1982100	93565	−0.10102	0.15964	−2302060	−1637630
Sample 3	−1985410	92553	−0.0233	0.12298	−2325000	−1632300
Sample 4	−1980010	86823	−0.28028	0.75853	−2412110	−1657230
Sample 5	−1986780	90776	−0.05874	0.20562	−2316480	−1633210
Sample 6	−1993140	89244	−0.16064	0.17712	−2380800	−1677460
Sample 7	−1987410	91865	−0.28757	0.89180	−2553190	−1685600
Sample 8	−1985370	85843	−0.13573	0.38890	−2362630	−1538990
Sample 9	−1995940	87631	−0.23869	0.65880	−2479220	−1652330
Sample 10	−1977210	89291	−0.05338	0.23054	−2303600	−1516040

Table 20: Statistics of 10 samples parameters of low tower in the system top node 874# Ux displacement time history under wind field 2 (m).

Displacement	Mean	SD	Skewness	Kurtosis	Minimum	Maximum
Sample 1	0.20474	0.01716	0.21285	−0.25034	0.15718	0.26938
Sample 2	0.19786	0.01478	−0.18439	−0.02441	0.14613	0.24476
Sample 3	0.19756	0.01429	0.6389	1.95256	0.15665	0.29188
Sample 4	0.19713	0.01639	0.25773	0.50871	0.14560	0.27491
Sample 5	0.20114	0.01573	0.23138	−0.07892	0.15503	0.26071
Sample 6	0.20166	0.01705	0.24128	0.67868	0.15298	0.28411
Sample 7	0.20188	0.01491	0.16281	0.67360	0.15510	0.27966
Sample 8	0.20029	0.01518	0.06761	0.09526	0.13861	0.26583
Sample 9	0.20143	0.01667	−0.09939	−0.02418	0.15240	0.2647
Sample 10	0.20109	0.01560	−0.08412	−0.13405	0.13951	0.24841

Table 21: Statistics of 10 samples parameters of low tower in the system element 3986# axial force time history under wind field 2 (N).

Axial force	Mean	SD	Skewness	Kurtosis	Minimum	maximum
Sample 1	−2003970	81613	−0.25174	−0.12699	−2393590	−1773560
Sample 2	−1970750	70321	0.21342	0.26403	−2201780	−1631920
Sample 3	−1970020	67161	−0.72856	2.71910	−2458630	−1755420
Sample 4	−1968010	76148	−0.3753	1.31182	−2458310	−1690060
Sample 5	−1989460	75171	−0.19104	0.12478	−2306520	−1698410
Sample 6	−1991600	78931	−0.28651	1.12501	−2457960	−1753990
Sample 7	−1990110	69899	−0.30044	1.64027	−2464100	−1734350
Sample 8	−1983460	70168	−0.06092	0.77690	−2364690	−1583980
Sample 9	−1989120	78892	0.02409	0.28657	−2373170	−1728910
Sample 10	−1985380	74337	0.10206	0.12704	−2228420	−1593240

Table 22: Comparison of statistical results on single high tower node 35# Ux displacement and element 1972# axial force.

Number	Statistical methods	Single high tower			
		Wind field 1		Wind field 2	
		Displacement (m)	Axial force (N)	Displacement (m)	Axial force (N)
1	Method 1	0.60214	−3783277	0.47170	−3375352
2	Method 2	0.55944	−3622471	0.45836	−3336793
3	Method 3	0.36013	−2947645	0.35139	−2928202
4	The average of mean	0.35353	−2938821	0.34950	−2924127
5	Item 1/Item 4	1.703	1.287	1.350	1.154
6	Item 2/Item 4	1.582	1.233	1.311	1.141
7	Item 3/Item 4	1.019	1.003	1.005	1.001

Table 23: Comparison of statistical results on single low tower node 874# Ux displacement and element 3986# axial force.

Number	Statistical methods	Single low tower			
		Wind field 1		Wind field 2	
		Displacement (m)	Axial force (N)	Displacement (m)	Axial force (N)
1	Method 1	0.38756	−2683970	0.31304	−2461538
2	Method 2	0.35570	−2575358	0.30012	−2409227
3	Method 3	0.22547	−2082638	0.22321	−2082823
4	The average of mean	0.22095	−2075966	0.22167	−2079914
5	Item 1/Item 4	1.754	1.293	1.412	1.183
6	Item 2/Item 4	1.610	1.241	1.354	1.158
7	Item 3/Item 4	1.020	1.003	1.007	1.001

Table 24: Comparison of statistical results on high tower in the system node 35# Ux displacement and element 1972# axial force.

Number	Statistical methods	High tower in transmission tower-line system			
		Wind field 1		Wind field 2	
		Displacement (m)	Axial force (N)	Displacement (m)	Axial force (N)
1	Method 1	0.43429	−3171906	0.40952	−3109766
2	Method 2	0.41255	−3117028	0.39069	−3048073
3	Method 3	0.32309	−2764258	0.32169	−2758864
4	The average of mean	0.32167	−2761720	0.32084	−2754673
5	Item 1/Item 4	1.35	1.15	1.28	1.13
6	Item 2/Item 4	1.28	1.13	1.22	1.11
7	Item 3/Item 4	1.00	1.001	1.00	1.00

Table 25: Comparison of statistical results on low tower in the system node 874# Ux displacement and element 3986# axial force.

Number	Statistical methods	Low tower in transmission tower-line system			
		Wind field 1		Wind field 2	
		Displacement (m)	Axial force (N)	Displacement (m)	Axial force (N)
1	Method 1	0.28247	−2392195	0.26844	−2370717
2	Method 2	0.26171	−2256128	0.24781	−2206980
3	Method 3	0.20194	−1988296	0.20110	−1985582
4	The average of mean	0.20092	−1986258	0.20048	−1984188
5	Item 1/Item 4	1.40	1.20	1.34	1.20
6	Item 2/Item 4	1.30	1.14	1.24	1.11
7	Item 3/Item 4	1.00	1.00	1.00	1.001

(2) The sample length of 600 s, 10 samples, and the number of statistical points 59,000 were selected to satisfy the accuracy of calculation results of the displacement and the axial force of the single tower and tower-line system. The frequency histograms of samples basically follow the Gaussian distribution. The characteristic statistical parameters of the samples are random.

(3) The results of the dynamic response of single towers and the transmission tower-line system show that the data obtained by Method 3 are closer to the average of the mean value. In the other two methods, for the single high tower under wind field 1, the displacements are 58%–70% larger than the average of mean, and the axial forces are 23%–29% larger than the average of mean values. Under the wind field 2, the displacements were 31%–35% larger than the average of mean, and the axial forces were 14%-15% larger as well. In the case of the single low tower under wind field 1, the displacements are 61%–75% larger than the average of mean, while the axial forces are 24%–29% larger. Under the wind field 2, the displacements were 35%–41% larger, and the axial forces were 16%–18% larger than the average of mean values.

(4) For the high tower in the system under wind field 1, the displacements are 28%–35% larger, and the axial forces are 13%–15% larger than their average of mean values. Under the wind field 2, the displacements were 22%–28% larger than the average of mean, and the axial forces exceeded on 11%–13% the average of mean values. For the low tower in the system, under wind field 1, the displacements are 30%–40% larger, while the axial forces are 14%–20% larger than the average of mean. And under the wind field 2, the displacements were 24%–34% larger than the average of mean; the axial forces were 11%–20% larger than the average of mean.

(5) The effect of statistical results of the low tower is greater than those of the high tower. The values obtained with wind field 1 is slightly larger than those under wind field 2, indicating that wind field 1 is more conservative than wind field 2. The results of the tower-line system are smaller than those of the single towers, which shows that the transmission line damps the transmission tower-line vibrations. The extended dynamic response statistical analysis should be carried out for the transmission tower-line system.

Conflicts of Interest

The authors declare that there are no conflicts of interest regarding the publication of this paper.

Acknowledgments

The authors gratefully acknowledge the financial support from Northeast Electric Power University (BSJXM-201521), Jilin City Science and Technology Bureau (20166012), and Natural Science Foundation of China (51378095).

References

[1] S. Ozono and J. Maeda, "In-plane dynamic interaction between a tower and conductors at lower frequencies," *Engineering Structures*, vol. 14, no. 4, pp. 210–216, 1992.

[2] N. Prasad Rao and V. Kalyanaraman, "Non-linear behaviour of lattice panel of angle towers," *Journal of Constructional Steel Research*, vol. 57, no. 12, pp. 1337–1357, 2001.

[3] R. C. Battista, R. S. Rodrigues, and M. S. Pfeil, "Dynamic behavior and stability of transmission line towers under wind forces," *Journal of Wind Engineering & Industrial Aerodynamics*, vol. 91, no. 8, pp. 1051–1067, 2003.

[4] H. Yasui, H. Marukawa, Y. Momomura, and T. Ohkuma, "Analytical study on wind-induced vibration of power transmission towers," *Journal of Wind Engineering & Industrial Aerodynamics*, vol. 83, pp. 431–441, 1999.

[5] G. Diana, M. Falco, A. Cigada, and A. Manenti, "On the measurement of over head transmission lines conductor self-damping," *IEEE Transactions on Power Delivery*, vol. 15, no. 1, pp. 285–292, 2000.

[6] T. Takahashi, T. Ohtsu, M. F. Yassin, S. Kato, and S. Murakami, "Turbulence characteristics of wind over a hill with a rough surface," *Journal of Wind Engineering & Industrial Aerodynamics*, vol. 90, no. 12, pp. 1697–1706, 2002.

[7] T. Okamura, T. Ohkuma, E. Hongo, and H. Okada, "Wind response analysis of a transmission tower in a mountainous area," *Journal of Wind Engineering & Industrial Aerodynamics*, vol. 91, no. 1, pp. 53–63, 2003.

[8] M. J. Paluch, T. T. O. Cappellari, and J. D. Riera, "Experimental and numerical assessment of EPS wind action on long span transmission line conductors," *Journal of Wind Engineering & Industrial Aerodynamics*, vol. 95, no. 7, pp. 473–492, 2007.

[9] T. G. Mara and H. P. Hong, "Effect of wind direction on the response and capacity surface of a transmission tower," *Engineering Structures*, vol. 57, pp. 493–501, 2013.

[10] W. G. Yang, K. Zhang, Z. Q. Wang, and Y. Q. Ge, "The influence of initial guy cable prestress on single-mast guyed tower's mechanical properties," *Applied Mechanics and Materials. Trans Tech Publications*, vol. 351, pp. 55–60, 2013.

[11] W. G. Yang, B. W. Zhu, and Z. Q. Wang, "Wind-induced response of UHV guyed single-mast transmission tower-line system," *Applied Mechanics and Materials*, vol. 501-504, pp. 533–537, 2014.

[12] B. Chen, W. H. Guo, P. Y. Li, and W. P. Xie, "Dynamic responses and vibration control of the transmission tower-line system: a state-of-the-art-review," *The Scientific World Journal*, vol. 2014, Article ID 538457, 20 pages, 2014.

[13] H. Aboshosha and A. El Damatty, "Engineering method for estimating the reactions of transmission line conductors under downburst winds," *Engineering Structures*, vol. 99, pp. 272–284, 2015.

[14] C. Zhou and Y. Liu, "Analytical model of high-voltage transmission line subjected to the downburst wind with rainfall," *Advances in Mechanical Engineering*, vol. 7, no. 3, pp. 1–13, 2015.

[15] C. Zhou, Y. Liu, and Z. Ma, "Investigation on aerodynamic instability of high-voltage transmission lines under rain-wind condition," *Journal of Mechanical Science and Technology*, vol. 29, no. 1, pp. 131–139, 2015.

[16] A. Hamada, "Nonlinear formulation of four-noded cable element and application to transmission lines under tornadoes," in *Proceedings of International conference on advances in wind and structures*, Busan, Korea, 2014.

[17] A. Hamada, *Numerical and Experimental Studies of Transmission Lines Subjected to Tornadoes [Ph.D. thesis]*, School of Graduate and Postdoctoral Studies, University of Western Ontario, 2014.

[18] A. Hamada and A. A. El Damatty, "Failure analysis of guyed transmission lines during F2 tornado event," *Engineering Structures*, vol. 85, pp. 11–25, 2015.

[19] A. Hamada and A. A. El Damatty, "Behaviour of transmission line conductors under tornado wind," *Wind and Structures, An International Journal*, vol. 22, no. 3, pp. 369–391, 2016.

[20] A. Hamada, J. P. C. King, A. A. El Damatty, G. Bitsuamlak, and M. Hamada, "The response of a guyed transmission line system to boundary layer wind," *Engineering Structures*, vol. 139, pp. 135–152, 2017.

[21] L. Tian and Y. Zeng, "Parametric study of tuned mass dampers for long span transmission tower-line system under wind loads," *Shock and Vibration*, vol. 2016, Article ID 4965056, 11 pages, 2016.

[22] C. D. F. Barbosa, C. Severino, E. Matsumoto et al., "Windbreaks working as barriers to high speed winds for protection of electric power transmission lines and towers," *Engineering Failure Analysis*, vol. 82, pp. 753–764, 2017.

[23] "Structural Design Concepts for Earthquake and Wind[S]," Architectural Institute of Japan, 1999.

[24] M. Gui-niu, *Research on wind-induced vibration time-history analysis of tall building structure[D]*, University of Technology, South China, Guangdong, China, 2010.

[25] A. G. Davenport, "The spectrum of horizontal gustiness near the ground in high winds," *Quarterly Journal of the Royal Meteorological Society*, vol. 87, no. 372, pp. 194–211, 1961.

[26] GB50009, *Load code for the design of Building structures [S]*, China Architecture and Building Press, Beijing, China, 2012.

[27] J. C. Kaimal, J. C. Wyngaard, Y. Izumi, and O. R. Coté, "Spectral characteristics of surface-layer turbulence," *Quarterly Journal of the Royal Meteorological Society*, vol. 98, no. 417, pp. 563–589, 1972.

[28] M. Shiotani and H. Arai, "Lateral Structures of Gusts in High Winds [C]," in *Proceedings of Conference on Wind*, pp. 20–26, University of Toronto Press, 1967.

[29] J. S. Owen, B. J. Eccles, B. S. Choo, and M. A. Woodings, "The application of auto-regressive time series modelling for the: time-frequency analysis of civil engineering structures," *Engineering Structures*, vol. 23, no. 5, pp. 521–536, 2001.

[30] Northeast Electric Power Design Institute of the National Electricity Company, *Power engineering high voltage power transmission line Design Manual*, China Electric Power Press, Beijing, China, 2003.

[31] X. Ruiguo, *Probability theory and mathematical statistics[M]*, Higher Education Press, Beijing, China, 2002.